JACS
JOURNAL OF THE AMERICAN CHEMICAL SOCIETY
Communication
pubs.acs.org/JACS

Surface-Supported Supramolecular Pentamers

Sujoy Karan,*[,†] Yongfeng Wang,*[,‡] Roberto Robles,[¶,§] Nicolás Lorente,[¶,§] and Richard Berndt[†]

[†]Institut für Experimentelle und Angewandte Physik, Christian-Albrechts-Universität zu Kiel, 24098 Kiel, Germany

[‡]Key Laboratory for the Physics and Chemistry of Nanodevices, Department of Electronics, Peking University, Beijing 100871, P.R. China

[¶]ICN2—Institut Catala de Nanociencia i Nanotecnologia and [§]CSIC—Consejo Superior de Investigaciones Cientificas, ICN2 Building, Campus de la Universitat Autònoma de Barcelona, 08193 Bellaterra, Barcelona, Spain

Supporting Information

ABSTRACT: Chiral pentamers of *all-trans*-retinoic acid molecules have been prepared on Au(111) surfaces and on a molecular monolayer. Over a range of coverages, pentamers are the building blocks of larger arrays that become increasingly enantiopure. The stability of pentamers is analyzed from experiments on an isomer and a more reactive substrate as well as from density functional theory. The linear shape of the molecule and suitable densities are crucial for the formation of pentamers, driven by cyclic hydrogen bonding between carboxylic acid moieties.

Supramolecular chemistry is of great interest in molecular recognition, catalysis, medicine, data storage and processing, and artificial photosynthetic devices.[1] Supramolecules are formed by directional and weak non-covalent interactions such as hydrogen bonding,[2] metal coordination,[3] hydrophobic and van der Waals forces,[4] and $\pi-\pi$ and electrostatic interactions.[5] Hydrogen bonding is particularly attractive for self-assembly for its directionality, specificity, and biological relevance.[6]

On surfaces, supramolecular structures are affected by direct interactions with the substrate.[7] In addition, substrate-mediated long-range molecule—molecule interactions occur and lead to discrete supramolecules instead of closely packed molecular arrays. Supramolecular dimers, trimers, and tetramers of porphyrines and azobenzene derivates have been self-assembled using these principles.[8] However, the fabrication of supramolecules with C_5 symmetry, which are mainly found in living organisms, has rarely been reported,[9] most likely because a two-dimensional surface cannot be filled with a periodic arrangements of pentagons.[10]

Here we present the preparation of supramolecular pentamers from *all-trans*-retinoic acid (ReA) on the Au(111) surface. Over a range of coverages these pentamers are the building blocks of larger arrays. While the ReA molecules, which become chiral upon adsorption, form a racemic mixture, the pentamers become increasingly enantiopure as larger arrays form. Using a slightly different molecule, 13-*cis*-retinoic acid (*cis*-ReA), or a more reactive substrate, Ag(111), we identify the forces driving the pentamer formation. Density functional theory (DFT) calculations are used to further characterize the process.

ReA was sublimated onto Au(111) at room temperature in ultrahigh vacuum. Images were recorded with a scanning tunneling microscope (STM) operated at 5 K, low constant currents (10—60 pA), and low positive sample voltages (10—150 mV). Molecular double layers were imaged at 2.1 V. Images are displayed as an illuminated three-dimensional surface.

Electronic structure calculations were performed within DFT using a plane wave basis set and the projector augmented wave method.[12] The exchange and correlation energy was treated with the Perdew-Burke-Ernzerhof (PBE) form of the generalized gradient approximation.[13] The importance of long-range van der Waals (vdW) interactions was studied using the DFT+D2 scheme of Grimme.[14] Geometries were optimized until forces were smaller than 0.01 eV/Å.

ReA is one of the most active retinoids and essential for the control of epithelial cell growth and cellular differentiation.[15] The molecule has a quasilinear geometry with the carboxyl group (—COOH) at one end. Figure 1a shows a STM image of a supramolecular pentamer that formed upon deposition of ReA on Au(111). As confirmed from DFT calculations the C_5 symmetric pentamer is stabilized by cyclic O···H—O hydrogen bonds at the center (Figure 1b). The bulky 1,3,3-trimethylcyclohexene groups appear as protrusions (0.2 nm apparent height) at the periphery of the supramolecular cluster while the chain-like rest of the molecules (3,7-dimethylnona-2,4,6,8-tetranoic acid, denoted oligoene below) appears lower (0.14 nm).

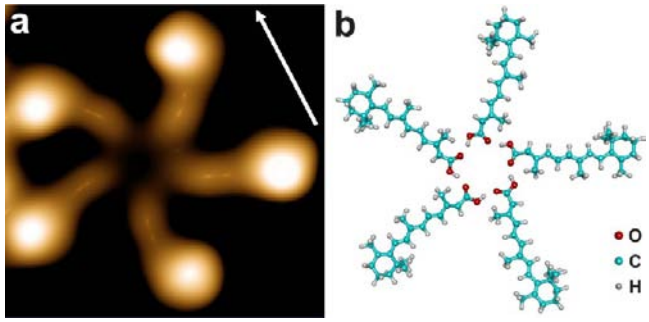

Figure 1. (a) Image of a ReA pentamer, observed close to a step on Au(111) at an average coverage $\Theta \approx 0.2$ ML.[11] In this and all other STM images an arrow indicates a $\langle 1\bar{1}0 \rangle$ direction and its length corresponds to 1.5 nm. (b) Optimized geometry of five ReA molecules, confined to a plane.

Received: May 31, 2013
Published: September 5, 2013

   dx.doi.org/10.1021/ja405456k | J. Am. Chem. Soc. 2013, 135, 14004—14007

At low coverages, most ReA molecules arrange themselves into pentamers which interact to form larger agglomerates, inititally in fcc areas of the herringbone reconstruction. While the pentamers can still easily be identified the C_5 symmetry is usually lost. We attribute the reduced symmetry to the van der Waals interaction between pentamers and the flexibility of the oligoene chains on Au(111). In fact, no preference for a particular crystallographic direction of the Au substrate was discernible, in stark contrast to a Ag(111) substrate (see below).

Close inspection of Figure 2a reveals that the surface induces a chirality of the achiral ReA molecule.[16] The two enantiomers,

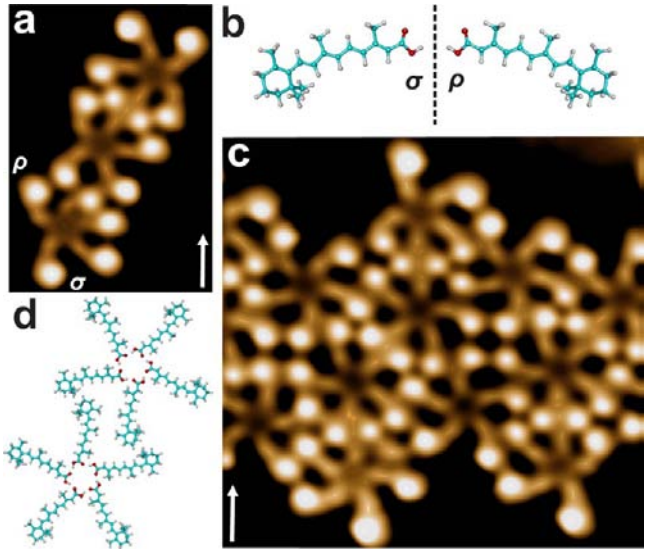

Figure 2. (a) STM image of three pentamers comprising different enantiomers of ReA at $\Theta \approx 0.4$ ML. ρ and σ indicate examples. (b) Surface-induced enantiomeric forms ρ and σ of ReA. (c) STM image of a larger pentamer array. (d) Schematic geometry of two pentamers attracted by van der Waals interaction.

denoted ρ and σ, are shown in Figure 2b. While small islands of a few pentamers (Figure 2a) comprise similar numbers of both enantiomers larger islands (Figures 2c and 3) exhibit a significant (~10:1) excess of one enantiomer. Most molecules with the minority chirality are found at the perimeter of islands. From an analysis of many islands we found that all pentamers that are surrounded by more than four neighboring pentamers are comprised of five identical enantiomers and thus are chiral themselves.[17] These observations indicate the importance of homochiral interactions. At coverages below 0.2 monolayer (ML[11]), ~5% of the pentamers are enantiopure as expected for random aggregation of σ and ρ enantiomers. This fraction increases to ~80% in pentamer islands at ~0.75 ML. The mechanism of enantioselectivity may be thermally induced chiral switching.[18] In such a process the bulky 1,3,3-trimethylcyclohexene groups would flip along the oligoene chains, thus change the handedness of the molecules and enable the growth of pentamers into homochiral extended islands.

Although a planar surface cannot be completely filled with regular pentagons Figure 3a shows that ReA pentamers are capable of forming large ordered arrays with a pattern resembling a pentagonal Cairo tiling.[19] Given the large size of the unit cell (black lines in Figure 3a), which comprises two pairs of pentamers, i.e., 20 molecules, the number of defects (yellow circles) of the structure is surprisingly low. This is attributed to a degree of flexibility of the pentamers, which adapt themselves to

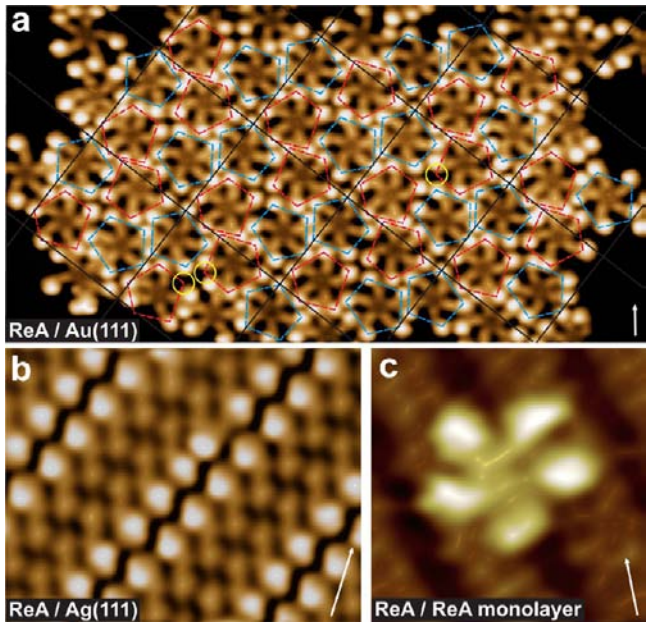

Figure 3. (a) STM image of ReA pentamers on Au(111) in a rectangular two-dimensional mesh at $\Theta \approx 0.75$ ML. Solid lines indicate some unit cells with dimensions 5.7×5.2 nm^2. The unit cell comprises four pentamers. Red and blue pentagons indicate pairs of pentamers with different distortions that are not congruent. The pentamers at the interior of the island contain only σ molecules. The two pentamers marked red (blue) are rotated by 180° with respect to each other. Defects in the interior of the pentamer array are marked with yellow circles. (b) ReA on Ag(111). The molecules form a densely packed, striped structure. The dimensions of the oblique unit cell are 3.6×0.82 nm^2 with an angle of $54 \pm 1°$ between the primitive vectors. (c) STM image of a pentamer grown on top of an ReA dimer island on Au(111) with monolayer thickness.

form a rectangular unit cell with two different pairs of distorted supermolecules. Moreover, the open structure of the periphery of the pentamers enables some interlocking with the ReA molecules from neighboring pentamers (cf. Figure 2d). From a pentagonal cyclooligomer a similar scenario was reported.[20] In that case, the intermolecular interactions attributed to interdigitating alkoxy substituents. Both cases are different from that of rigid pentagonal molecules where parallel and antiparallel linear packings and a so-called rotator phase have been reported.[21] In small arrays (Figures 2a and 2c), where most of the pentamers are part of the rim, the molecular orientations are less well ordered.

To address the role of the molecule−substrate interaction, we repeated the experiments on the more reactive Ag(111) surface, keeping all other parameters unchanged. On this surface, no pentamers were found over a wide range of coverages. Instead, densely packed islands were observed (Figure 3b). We attribute this striking difference between the Au and Ag substrates to the different strengths of the molecule−substrate interactions. Our calculations showed that intermolecular hydrogen bonding favors pentamer formation. On Au(111) the interaction with the substrate is too small to change this preference. On Ag(111), the corrugation of the interaction potential is more significant and imposes an alignment of the molecules along $\langle \bar{2}11 \rangle$ directions and thus effectively prevents the formation of pentamers.

From the above results it appears likely that ReA pentamers will form on other inert surfaces as well. As a first test of this idea,

dx.doi.org/10.1021/ja405456k | J. Am. Chem. Soc. 2013, 135, 14004−14007

a small amount of ReA was deposited on a complete ReA monolayer on Au(111). The geometric and electronic structures of this layer deviate significantly from those of the metallic Au(111) substrate. Nevertheless, pentamers were found on top of the molecular layer (Figure 3c) as expected.

To characterize the driving force for pentamer formation the structure of ReA clusters was calculated using DFT. To keep the calculation tractable, the interaction with the fairly inert Au(111) surface was neglected but the molecules were confined to two dimensions. This simplification is justified for the following reasons (cf. also Supporting Information S2). First, the ReA molecules in pentamers were not observed to exhibit a clear preference for a particular crystallographic direction of the substrate. On the more reactive but structurally similar Ag(111) surface no pentamers were found and the ReA molecules are aligned with respect to the substrate. Second, at elevated coverages the pentamer islands extend over fcc and hcp areas as well as domain walls of the herringbone reconstruction without significant changes of the molecular arrangement.

Calculated binding energies $E(n)$ of cyclic clusters of $n = 2-6$ molecules are displayed in Table 1. With increasing cluster size, the binding energy E^{PBE} calculated with the PBE functional continuously grows up to a magic size $n = 5$. Most of the binding of the clusters is due to O···H−O bonds. The energy per O···H−O bond is higher for the dimer (0.43 eV), which can be tracked to an angle closer to 180° and a shorter distance. When adding more molecules, additional H-bonds are formed, but they are weaker because of the spatial restrictions of accommodating the consecutive molecules. That leads to a less open bond (farther from 180°) with larger distances. Finally, the addition of the sixth molecule lowers the energy per dangling bond so much that there is an overall reduction in binding energy, inhibiting the formation of the hexamer and stopping the process at the pentamer. At lower coverages the process is governed by kinetics and pentamers are formed, but a higher coverages the most stable structures per H-bond are formed, i.e., dimer networks (see below). van der Waals interactions ($E^{PBE+vdW}$) further increase the binding energy and do not change the overall trend. Hexamers turn out to be significantly less stable. These results show that the attachment of single ReA molecules to existing clusters is favorable until a pentamer is formed. While fission of pentamers into smaller clusters would lead to a gain of energy, the abundance of pentamers in the experiments shows that this process is inefficient. This indicates that the barrier for fission is significant.

Table 1. Calculated Binding Energies, in eV (= 96.485 kJ/mol), of Enantiopure ReA Clusters[a]

n	E^{PBE}	$E^{PBE+vdW}$	$\Delta_{2,n}^{PBE+vdW}$
2	0.76	0.85	0.69
3	0.88	1.01	−0.05
4	0.96	1.23	−0.01
5	1.00	1.45	0.84/0.53
6	0.22/0.68	0.83/1.15	–

[a]For the hexamer, the first value was found for a cyclic arrangement that is obtained by inserting a sixth molecule into a pentamer. The second, higher binding energy corresponds to a different structure (see Figure S1) that would require a drastic rearrangement of the pre-existing pentamer. The quantity in the right column shows the relative stability (details in the text) of respective clusters.

The formation of pentamer arrays as the one shown in Figure 3a was also found to be energetically favorable. We have checked several packing configurations of pentamers, finding that the binding energy per pentamer increases due to the pentamer−pentamer interactions, going up to 1.85 eV in the best of the tested cases.

The effect of the molecular coverage on the formation of pentamers has been systematically investigated in the experiments (additional STM images are shown in Figure S2). Pentamers were the most abundant structural motif in the range 0.01 ML < Θ < 0.4 ML although decreasing percentages of pentamers were observed up to Θ ≈ 1 ML. At densities exceeding half a monolayer, ordered islands form. They may be viewed as being comprised of supramolecular tetramers (Figure 4a) or dimers (Figure 4b). Optimized geometries of these building blocks are overlaid on the respective STM images. Close to 1 ML, the Au(111) substrate is mostly covered with the dimer pattern of Figure 4b. This is consistent with the results of Table 1, which show that the binding energy per ReA molecule is maximal in dimers. To theoretically characterize the interaction between dimers a monolayer in the configuration of Figure 4b was considered. We found a binding energy of 1.51 eV per dimer, considerably larger than the binding energy of an isolated dimer. At coverages below 0.01 ML, we occasionally observed trimers (see Figure S3). This may be understood from their low stability compared to dimers and tetramers. In Table 1 the relative stability is indicated by the quantity $\Delta_{2,n} = 2E(n) - E(n+1) - E(n-1)$.[22] The larger negative value of the trimers shows their instability. Again, dimers and pentamers are the more stable formations.

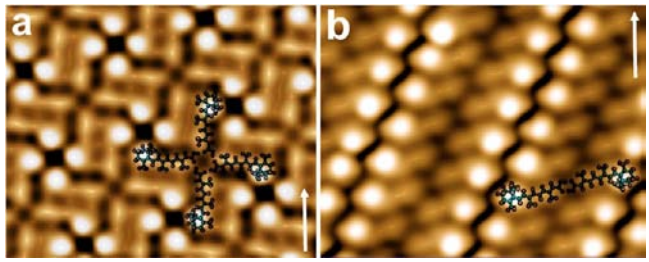

Figure 4. STM images of dense patterns observed on Au(111) at elevated coverages. (a) Pattern comprisng ReA tetramers. (b) Striped pattern comprising ReA dimers. The molecules within a given island exhibit the same handedness. Different islands may exhibit different chiralities. Optimized models of a tetramer and a dimer are overlaid.

Finally, we experimentally address the role of the shape of the ReA molecule. To this end the closely related molecule *cis*-ReA (Figure 5a) was deposited on Au(111) and Ag(111). On both substrates, hexagonal networks of H-bonded dimers were found and pentamers were absent. Figure 5b shows an example on Au(111). This result highlights the relevance of the linear shape of the ReA molecule. In the case of *cis*-ReA, steric hindrance suppresses the formation of closed cycles of O···H−O hydrogen bonds. This is particularly important during the growth process when molecules with different chiralities try to attach to a ReA_n, $n < 5$ cluster. Whereas ReA pentamers containing different enantiomers are stable owing to the linear shape of the constituents (Figure 5c), closure of the cyclic hydrogen bond pattern is prevented in *cis*-ReA tetramers when a molecule with different chirality is added (Figure 5d). The calculated binding energies of heterochiral (Figure 5c) and homochiral (Figure 1b) ReA pentamers, 1.42 and 1.45 eV, respectively, are similar

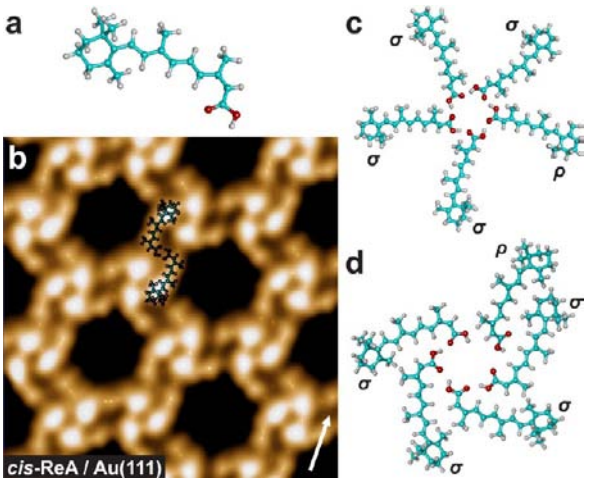

Figure 5. (a) Structure of *cis*-ReA. (b) STM image of a hexagonal network formed by *cis*-ReA on Au(111). A virtually identical structure was observed on Ag(111). An optimized molecular dimer is overlaid on the STM image. (c,d) Optimized heterochiral pentamers of ReA and *cis*-ReA, respectively.

although homochirality appears to be slightly favored. This is consistent with the observation of coexisting homo- and heterochiral ReA pentamers.

In conclusion, pentamers of *all-trans*-retinoic acid molecules have been prepared on the pristine Au(111) surface and a molecular monolayer. Cycles of hydrogen bonds between carboxylic acid moieties stabilize the pentamers. The linear shape of ReA and suitable molecular densities are crucial for pentamer formation. We speculate that related self-assembly of pentamers may be achieved on other weakly interacting surfaces.

■ ASSOCIATED CONTENT

Ⓢ Supporting Information

Role of the substrate; optimized geometries of ReA hexamers; overview images of ReA on Au(111); ReA trimer on Au(111). This material is available free of charge via the Internet at http://pubs.acs.org.

■ AUTHOR INFORMATION

Corresponding Authors

karan@physik.uni-kiel.de

yongfengwang@pku.edu.cn

Notes

The authors declare no competing financial interest.

■ ACKNOWLEDGMENTS

We acknowledge Centre of Supercomputing of Galicia (CESGA) for computational resources. Financial support by the Deutsche Forschungsgemeinschaft through SFB 677 and the Ministry of Science and Technology of China (2013CB933404) is acknowledged.

■ REFERENCES

(1) (a) Bartels, L. *Nature Chem.* **2010**, *2*, 87. (b) Barth, J. V. *Annu. Rev. Phys. Chem.* **2007**, *58*, 375.

(2) (a) Pawin, G.; Wong, K. L.; Kwon, K.-Y.; Bartels, L. *Science* **2006**, *313*, 961. (b) Ye, Y.; Sun, W.; Wang, Y.; Shao, X.; Xu, X.; Cheng, F.; Li, J.; Wu, K. *J. Phys. Chem. C* **2007**, *111*, 10138. (c) Otero, R.; Lukas, M.; Kelly, R. E. A.; Xu, W.; Lægsgaard, E.; Stensgaard, I.; Kantorovich, L. N.; Besenbacher, F. *Science* **2008**, *319*, 312. (d) Griessl, S.; Lackinger, M.; Edelwirth, M.; Hietschold, M.; Heckl, W. M. *Single Mol.* **2002**, *3*, 25. (e) Stöhr, M.; Wahl, M.; Galka, C. H.; Riehm, T.; Jung, T. A.; Gade, L. H. *Angew. Chem., Int. Ed.* **2005**, *44*, 7394. (f) De Feyter, S.; De Schryver, F. C. *Chem. Soc. Rev.* **2003**, *32*, 139.

(3) (a) Langner, A.; Tait, S. L.; Lin, N.; Rajadurai, C.; Ruben, M.; Langner, A.; Kern, K. *Proc. Natl. Acad. Sci. U.S.A.* **2007**, *104*, 17927. (b) Lin, T.; Shang, X. S.; Adisoejoso, J.; Liu, P. N.; Lin, N. *J. Am. Chem. Soc.* **2013**, *135*, 3576. (c) Shi, Z.; Lin, N. *J. Am. Chem. Soc.* **2009**, *131*, 5376.

(4) Qiu, X.; Wang, C.; Zeng, Q.; Xu, B.; Yin, S.; Wang, H.; Xu, S.; Bai, C. *J. Am. Chem. Soc.* **2000**, *122*, 5550.

(5) (a) Böhringer, M.; Schneider, W.-D.; Berndt, R. *Angew. Chem., Int. Ed.* **2000**, *39*, 792. (b) Wong, K.; Kwon, K.-Y.; Rao, B. V.; Liu, A.; Bartels, L. *J. Am. Chem. Soc.* **2004**, *126*, 7762. (c) deWild, M.; Berner, S.; Suzuki, H.; Yanagi, H.; Schlettwein, D.; Ivan, S.; Baratoff, A.; Guentherodt, H.-J.; Jung, T. A. *ChemPhysChem* **2002**, *3*, 881.

(6) (a) Kühnle, A.; Linderoth, T. R.; Hammer, B.; Besenbacher, F. *Nature* **2002**, *415*, 891. (b) Mao, X.-B.; Wang, C.-X.; Wu, X.-K.; Ma, X.-J.; Liu, L.; Zhang, L.; Niu, L.; Guo, Y.-Y.; Li, D.-H.; Yang, Y.-L.; Wang, C. *Proc. Natl. Acad. Sci. U.S.A.* **2011**, *108*, 19605.

(7) Lukas, S.; Witte, G.; Wöll, C. *Phys. Rev. Lett.* **2002**, *88*, 028301.

(8) (a) Wang, Y.; Ge, X.; Schull, G.; Berndt, R.; Bornholdt, C.; Koehler, F.; Herges, R. *J. Am. Chem. Soc.* **2008**, *130*, 4218. (b) Yokoyama, T.; Yokoyama, S.; Kamikado, T.; Okuno, Y.; Mashiko, S. *Nature* **2001**, *413*, 619. (c) Yokoyama, T.; Kamikado, T.; Yokoyama, S.; Mashiko, S. *J. Chem. Phys.* **2004**, *121*, 11993. (d) Wang, Y.; Ge, X.; Manzano, C.; Kröger, J.; Berndt, R.; Hofer, W. A.; Tang, H.; Cerda, J. *J. Am. Chem. Soc.* **2009**, *131*, 10400.

(9) (a) Blüm, M.-C.; Ćavar, E.; Pivetta, M.; Patthey, F.; Schneider, W.-D. *Angew. Chem., Int. Ed.* **2005**, *44*, 5334. (b) Écija, D.; Urgel, J. I.; Papageorgiou, A. C.; Joshi, S.; Auwärter, W.; Seitsonen, A. P.; Klyatskaya, S.; Ruben, M.; Fischer, S.; Vijayaraghavan, S.; Reichert, J.; Barth, J. V. *Proc. Natl. Acad. Sci. U.S.A.* **2013**, *110*, 6678.

(10) (a) Pivetta, M.; Blüm, M.-C.; Patthey, F.; Schneider, W.-D. *Angew. Chem.* **2008**, *120*, 1092. (b) Bauert, T.; Merz, L.; Bandera, D.; Parschau, M.; Siegel, J. S.; Ernst, K.-H. *J. Am. Chem. Soc.* **2009**, *131*, 3460.

(11) We define 1 ML as the coverage of the most dense structure observed, Figure 4b.

(12) (a) Kresse, G.; Furthmüller, J. *Comput. Mater. Sci.* **1996**, *6*, 15. (b) Kresse, G.; Joubert, D. *Phys. Rev. B* **1999**, *59*, 1758.

(13) Perdew, J. P.; Burke, K.; Ernzerhof, M. *Phys. Rev. Lett.* **1996**, *77*, 3865.

(14) Grimme, S. *J. Comput. Chem.* **2006**, *27*, 1787.

(15) (a) Strickland, S.; Mahdavi, V. *Cell* **1978**, *15*, 393. (b) Shubeita, H. E.; Sambrook, J. F.; Mccormick, A. M. *Proc. Natl. Acad. Sci. U.S.A.* **1987**, *84*, 5645.

(16) (a) Barlow, S. M.; Raval, R. *Surf. Sci. Rep.* **2003**, *50*, 201. (b) Ernst, K.-H. *Top. Curr. Chem.* **2006**, *265*, 209.

(17) (a) Böhringer, M.; Morgenstern, K.; Schneider, W.-D.; Berndt, R.; Mauri, F.; Vita, A. D.; Car, R. *Phys. Rev. Lett.* **1999**, *83*, 324. (b) Gopakumar, T. G.; Matino, F.; Schwager, B.; Bannwarth, A.; Tuczek, F.; Kröger, J.; Berndt, R. *J. Phys. Chem. C* **2010**, *114*, 18247.

(18) Weigelt, S.; Busse, C.; Petersen, L.; Rauls, E.; Hammer, B.; Gothelf, K. V.; Besenbacher, F.; Linderoth, T. R. *Nat. Mater.* **2006**, *5*, 112.

(19) Grünbaum, B.; Shephard, G. C. *Tilings and Patterns*; Freeman: New York, 1987.

(20) Jester, S.-S.; Sigmund, E.; Höger, S. *J. Am. Chem. Soc.* **2011**, *133*, 11062.

(21) (a) Tahara, K.; Balandina, T.; Furukawa, S.; De Feyter, S.; Tobe, Y. *CrystEngComm* **2011**, *13*, 5551. (b) Ren, C. L.; Zhou, F.; Qin, B.; Ye, R. J.; Shen, S.; Su, H. B.; Zeng, H. Q. *Angew. Chem., Int. Ed.* **2011**, *50*, 10612. (c) Guillermet, O.; Niemi, E.; Nagarajan, S.; Bouju, X.; Martrou, D.; Gourdon, A.; Gauthier, S. *Angew. Chem.* **2009**, *121*, 2004. (d) Zoppi, L.; Bauert, T.; Siegel, J. S.; Baldridge, K. K.; Ernst, K.-H. *Phys. Chem. Chem. Phys.* **2012**, *14*, 13365.

(22) Robles, R.; Khanna, S. N.; Castleman, J. *Phys. Rev. B* **2008**, *77*, 235441.